Preparation and Characterization of Ring-Shaped Co Nanomaterials

Lin Guo,*,† Fang Liang,† Ning Wang,*,† Desheng Kong,‡ Siming Wang,‡ Lin He,‡ Chinping Chen,*,‡ Xiangmin Meng,§ and Ziyu Wu*,||

School of Chemistry and Environment, Beijing University of Aeronautics and Astronautics, Beijing 100083, P. R. China, Department of Physics, Peking University, Beijing 100871, China, Laboratary of Optoelectronic Functional Materials and Molecular Engineering and Technical Institute of Physics and Chemistry, Chinese Academy of Sciences, Beijing 100080, China, and Institute of High Energy Physics, Chinese Academy of Science, Beijing 100039, China

Received September 11, 2007. Revised Manuscript Received May 30, 2008

Donut- or ring-shaped Co nanomaterials were successfully synthesized using the polymer-modified method, by which PVP is used as a surface modifier reagent. The synthesized products were structurally and morphologically characterized by X-ray diffraction (XRD), scanning electron microscopy (SEM), and transmission electron microscopy (TEM), whereas the magnetic characterization was performed by temperature- and field-dependent magnetization measurements. The results show that the rings have a h-Co nanostructure. The outer diameter is about 400−500 nm, inner diameter 150−250 nm, and the ring plane thickness ∼120 nm. The magnetization measurements show a typical coercivity of about 112 Oe at 300 K and an almost vanishing coercivity, $H_C \approx 0$ at $T = 5$ K. Numerical calculations using the packeage of object oriented micromagnetic framework (OOMMF) reveal a magnetization ground-state of flux closure structure, as expected for the geometric structure of the submicrometer-sized Co rings. This explains the observed hysteresis loops at low temperature with a vanishing small coercivity. A possible reaction process for the formation of the donut-shaped Co nanostructure is presented.

Introduction

Magnetic nanomaterials exhibit interesting properties with broad application potentials.[1] In particular, application in the high-density information storage devices is probably one of the most important examples. It requires that the magnetic elements are ferromagnetic at room temperature, separated spatially without the presence of a stray field coupling, and electrically isolated among them.[2] With these conditions, metallic cobalt and its derived compounds are proper candidates that exhibit important magnetic properties deserving a special attention. In addition to the electrical, optical and other characteristic properties, the size and shape of inorganic nanocrystals are important factors for application,[3–5] Therefore, a lot of efforts have been directed to the accurate control processes in tailoring the shape, size, dimensionality, and complexity of nanocrystals.[6] In this direction, submicrometer-sized or nanoscaled ferromagnetic cobalt with various morphologies, including particles,[7,8] tubes,[9,10] rods,[11,12] wires,[13–16] rings,[17] and even chains of hollow spheres[18,19] have been successfully synthesized. Accordingly, various synthesizing methods, such as the self-assembly, thermal decomposition, template, solid-state, chemical solution, and sol−gel methods, have been developed to grow magnetic Co nanomaterials. In particular, the chemical solution method is probably the simplest, most low-cost, and easiest to control.

Co nanoparticle rings have been obtained by the Tripp team via thermolysis of $Co_2(CO)_8$ in hot toluene solutions containing a surfactant.[17,20,21] With their procedure, ferromagnetic cobalt nanoparticles are self-assembled to form

* To whom correspondence should be addressed. E-mail: guolin@buaa.edu.cn (L.G.); cpchen@pku.edu.cn (C.C); wangning@mse.buaa.edu.cn (N.W.); wuzy@ihep.edu.cn (Z.W.)

† Beijing University of Aeronautics and Astronautics.

‡ Peking University.

§ Laboratary of Optoelectronic Functional Materials and Molecular Engineering and Technical Institute of Physics and Chemistry, Chinese Academy of Sciences.

|| Institute of High Energy Physics, Chinese Academy of Science.

(1) Rothman, J.; Klaui, M.; Lopez-Diaz, L.; Vaz, C. A. F.; Bleloch, A.; Bland, J. A. C.; Cui, Z.; Speaks, R. *Phys. Rev. Lett.* **2001**, *86*, 1098.
(2) Weller, D.; Moser, A. *IEEE Trans. Magn.* **1999**, *35*, 4423.
(3) Klein, D. L.; Roth, R.; Lim, A. K. L. *Nature* **1997**, *389*, 699.
(4) Lieber, C. M. *Solid State Commun.* **1998**, *107*, 607.
(5) Pan, Z. W.; Dai, Z. R.; Wang, Z. L. *Science* **2001**, *291*, 1947.
(6) Xia, Y. N.; Yang, P. D.; Sun, Y. G.; Wu, Y. Y.; Mayer, B.; Gates, B.; Yin, Y. D.; Kim, F.; Yan, H. *Adv. Mater.* **2003**, *15*, 353.
(7) Lisiecki, I.; Albouy, P.; Pileni, M. *Adv. Mater.* **2003**, *15*, 712.
(8) Flahaut, E.; Agnoli, F. *Chem. Mater.* **2002**, *14*, 2553.
(9) Ji, G.; Su, H.; Tang, S.; Du, Y.; Xu, B. *Chem. Lett.* **2005**, *34*, 86.
(10) Crowley, T. A.; Ziegler, K. J.; Lyons, D. M.; Erts, D.; Olin, H.; Morris, M. A.; Holmes, J. D. *Chem. Mater.* **2003**, *15*, 3519.
(11) Xu, F.; Bando, Y.; Golberg, D.; Hasegawa, M.; Mitome, M. *Acta Mater.* **2004**, *52*, 601.
(12) Aslam, M.; Bhobe, R.; Alem, N.; Donthu, S.; Dravid, V. P. *J. App. Phys.* **2005**, *98*, 074311.
(13) Qin, D.; Liu, M. H.; Li, *Chem. Phys. Lett.* **2001**, *350*, 51.
(14) Bantu, A.; Rivas, J.; Zaragoza, G.; López-Quintela, M. A.; Blanco, M. C. *J. Non-Cryst. Solids* **2001**, *287*, 5.
(15) Xu, J.; Huang, X.; Xie, G.; Fang, Y.; Liu, D. *Mater. Lett.* **2005**, *59*, 981.
(16) Vila, L.; Vincent, P.; Pra, L. D.; Pirio, G.; Minoux, E.; Gangloff, L.; Demoustier-Champagne, S.; Sarazin, N.; Ferain, E.; Legras, R.; Piraux, L.; Legagneux, P. *Nano Lett.* **2004**, *4*, 521.
(17) Tripp, S. L.; Pusztay, S. V.; Ribbe, A. E.; Wei, A. *J. Am. Chem. Soc.* **2002**, *124*, 7914.
(18) Guo, L.; Liang, F.; Wen, X. G.; Yang, S. H.; He, L.; Zheng, W. Z.; Chen, C. P.; Zhong, Q. P. *Adv. Funct. Mater.* **2007**, *17* (3), 425.
(19) Liang, F.; Guo, L.; Zhong, Q. P.; Wen, X. G.; Yang, S. H.; Zheng, W. Z.; Chen, C. P.; Zhang, N. N.; Chu, W. G. *Appl. Phys. Lett.* **2006**, *89* (10), 103105.
(20) Tripp, S. L.; Dunin-Borkowski, R. E.; Wei, A. *Angew. Chem., Int. Ed.* **2003**, *42* (45), 5591.

10.1021/cm7025784 CCC: $40.75
Published on Web 07/25/2008

bracelet-like rings with a discrete particle count when dispersed by *C*-undecylcalix[4] resorcinarene (1). Liu[22] and Yosef[23] have reported the synthesis of gold and silver rings by similar self-assembly process. More recently, J. J. Torres-Heredia et al., have investigated the magnetic states and switching processes of Co nanorings with lateral dimensions of 200 nm using micromagnetic simulations.[24]

There are a few reports on the synthesis of Co solid ring. Zhu have fabricated a large number ($\sim 1 \times 10^{-9}$) of Co nanoring with inner diameters of 100 nm and widths of 20 nm using a nanosphere-template method.[25] Here, we demonstrate a chemical solution method for the synthesis of the donut-shaped Co nanoparticles in a polymer solution. The advantages of the method lie in mild reaction conditions, low cost, and high yield.

Experimental Section

The chemical reagents used in the experiment were analytical grade and used without further purification. The donut-shaped products were synthesized with the following procedure. First, 0.0012 mol of $CoCl_2 \cdot 6H_2O$ and 0.012 mol of Poly(vinylpyrrolidone) (PVP, M_W 58 000) were dissolved in 60 mL of ethylene glycol (EG) by intensive stirring for 12 h to obtain a homogeneous transparent mauve solution. Then, 0.5 mL of hydrazine monohydrate (50% Vol. A.R.) was added dropwise to the well-stirred mixture at room temperature with a simultaneous vigorous agitation. The solution turned turbid and pink. The stirring process further continued for at least one more hour in order to gurantee a thorough reaction. The mixture was subsequently heated to the boiling point of ethylene glycol (EG) for refluxing (~470 K). Numerous bubbles were formed in the flask with an ammonia smell. After refluxing for 4 h, the color of the solution turns from pink to dark and finally a dark precipitate was achieved. The system was then slowly cooled to room temperature. The final product was collected by centrifugation and washed with absolute ethanol for six times to remove all ionic remnants, and then dried at 353 K to finally obtain a loose dark powder. These as-prepared products were later characterized.

X-ray powder diffraction (XRD, Rigaku, $D_{max}2200$, Cu-kα) was used for the structural determination. Further microstructural analyses were also performed using a scanning electron microscopy (SEM) (JSM-5800 with an accelerating voltage of 3.0 kV) and transmission electron microscopy (TEM) (JEOL 2100F). TEM samples were first prepared by dispersing powders in alcohol by ultrasonic treatment, then dropping the suspension onto a holey carbon film supported on a copper grid dried in air. Magnetic properties were measured using a Quantum Design SQUID magnetometer.

Results and Discussion

Figure 1 shows the XRD pattern of the donut-shaped Co products prepared with PVP as a surface modifier. In the figure, there are at least five peaks with 2θ values of 2.16, 2.02, 1.91, 1.25, and 1.06, corresponding to the (100), (002), (101), (110), and (112) crystal planes of pure Co, respectively. These data are in good agreement with the XRD reflections of hexagonal Co (JCPDS, 05−0727).

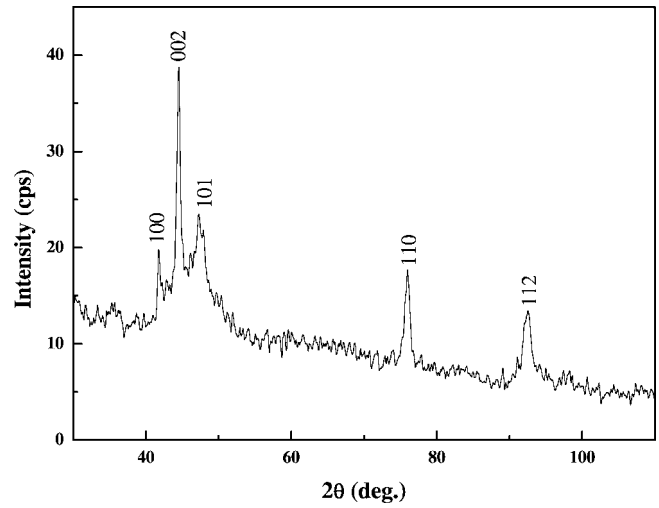

Figure 1. Typical XRD pattern of the Co products.

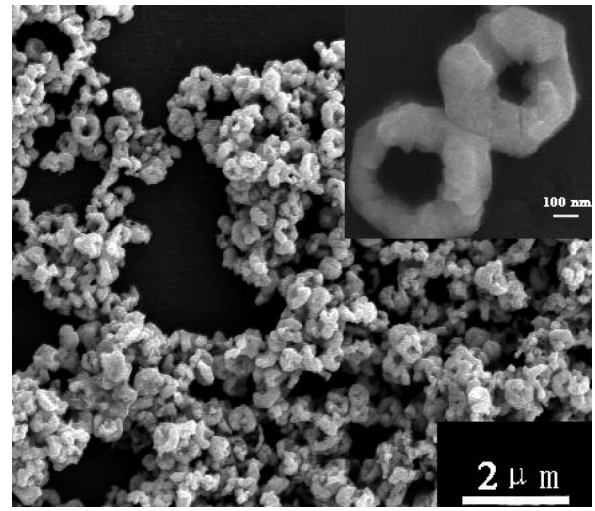

Figure 2. SEM image of donut-shaped Co nanoparticles.

A scanning electron microscopy (SEM) image of a representative sample is shown in Figure 2. It reveals a donut-shaped nanostructure for the sample with a thickness of about 120−150 nm. A more detailed SEM image for the Co rings at a higher magnifying factor is shown in the inset. It clearly reveals the donut-shaped structure for the Co nanorings, with a rough outer surface. Figure 3 shows the distribution of the interior and outer diameters of the Co nanorings. About 80% of the outer diameter ranges between 400 to 500 nm, and 95% of the interior diameter is between 150 and 250 nm.

The ring- or donut-shaped structure of the Co samples was further revealed by the transmission electron microscopy (TEM), shown in Figure 4. The outer diameter of the ring ranges from 400 to 500 nm. A typical TEM image of a single donut-shaped nanoparticles is shown in Figure 4b. Again, we clearly see that it is about 500 nm in diameter with a thickness of about 120 nm. Further information on the donut-shaped structure was obtained by the HRTEM technique. Figure 4c is a detailed view on the surface of the outer periphery. Images d and e in Figure 4 show views on the surfaces of the ring plane and the interior of the ring,

(21) Wei, A. *Chem. Commun.* **2006**, (15), 1581.
(22) Liu, Z.; Levicky, R. *Nanotechnology* **2004**, *15* (11), 1483.
(23) Yosef, G.; Rabani, E. *J. Phys. Chem. B* **2006**, *110* (42), 20965.
(24) Torres-Heredia, J. J.; Lo′ pez-Urı′ as, F.; M uñ oz-Sandoval, E. *J. Magn. Magn. Mater.* **2006**, *305* (1), 133.
(25) Zhu, F. Q.; Fan, D.; Zhu, X.; Zhu, J.; Cammarata, R. C.; Chien, C. *Adv. Mater.* **2004**, *16*, 23–24.

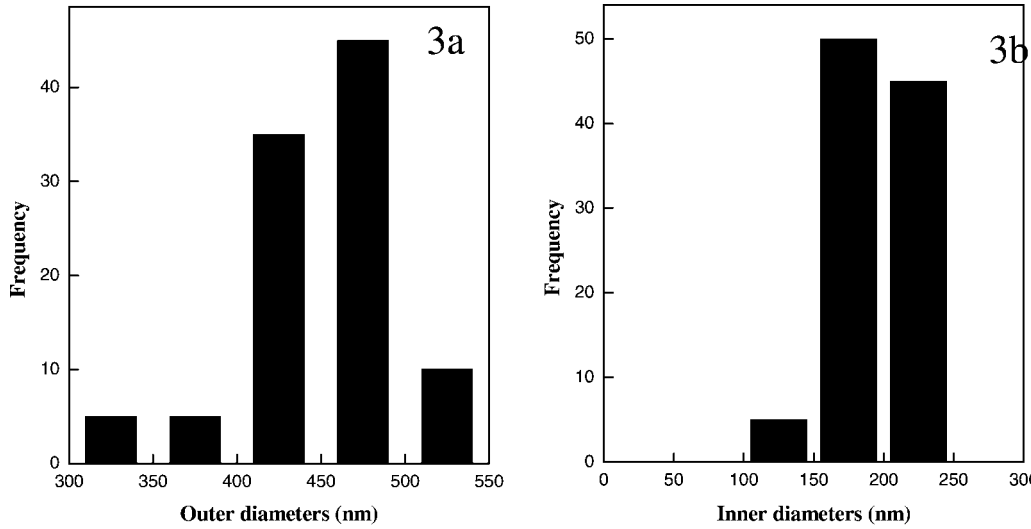

Figure 3. Distribution of the interior and outer diameters of the Co rings: (a) outer diameter, (b) interior diameter.

respectively. From the lattice fringes shown by these images, the interplanar spacing of 0.20 nm matches well with the distance of (002) crystal planes in hexagonal cobalt. There obviously exists a preferential growth direction and local area crystallinity. The lattice fringes prolongate across the entire surface of the ring without interruption by an apparent boundary.

The chemical reaction to produce the donut-shaped Co nanomaterials can be divided in several independent steps, including complexion, reduction, nucleation, and assembly in a multicomponent system. The reaction can be written as follows

$$Co^{2+} + 3N_2H_4 \rightarrow [Co(N_2H_4)_3]^{2+}$$

$$[Co(N_2H_4)_3]^{2+} + N_2H_4 \rightarrow Co\downarrow + 4NH_3\uparrow + 2N_2\uparrow + H_2\uparrow + 2H^+$$

Figure 5 illustrates a possible mechanism for the formation of the donut-shaped Co nanomaterials. In the beginning, Co^{2+} ions in the solution react with hydrazine to form a pink complex, $[Co(N_2H_4)_3]Cl_2$, which is very stable in ambient as previously observed.[26,27] When the pink solution is heated to the boiling point of ethylene glycol (EG) for refluxing (~470 K), reduction reaction occurs in the presence of excessive hydrazine to form numerous Co nanoparticles. With the PVP polymer chains wrapping around to form clusterlike aggregates in the solution,[28] the Co nanoparticles may be adsorbed on the surface of PVP clusters or micelles to reduce their surface energy. The formation of the Co ring thus takes place, as depicted by the illustration in Figure 5. After the PVP cores are washed away using absolute ethanol, the donut-shaped structures appear as observed.

Magnetic characterization of the powder sample was performed with a Quantum Design MPMS SQUID magnetometer. Magnetic simulation for these nanoelements was based on the package of object oriented micromagnetic framework (OOMMF) available from NIST.[29] The temperature-dependent magnetization, $M(T)$, of the sample was first studied by zero field cooling (ZFC) and field cooling (FC) $M(T)$ modes from 5 to 380 K. For the $M_{ZFC}(T)$ curve, the sample was first cooled to $T = 5$ K under zero applied field, and then the magnetization was recorded in an applied field, $H_{app} = 90$ Oe, in the warming process. For the $M_{FC}(T)$ curve, the procedure was the same, i.e., the data were recorded in the field of 90 Oe, except that the sample was cooled under an applied magnetic field of $H_{COOL} = 20$ kOe. The $M_{ZFC}(T)$ and $M_{FC}(T)$ curves are plotted in Figure 6. These two separate widely from each other with the temperature going up to 380 K. The difference in the magnetization, $\Delta M(T) = M_{FC}(T) - M_{ZFC}(T)$, reveals the presence of a magnetic anisotropy barrier.[30–32] The nonvanishing $\Delta M(T)$ at $T = 380$ K indicates that the blocking temperature exceeds the upper limit of temperature for the measurement at $T = 380$ K.

The $M(H)$ measurements were performed at $T = 5$ and 300 K, shown in panels a and b in Figure 7, respectively. The saturation magnetizations are almost equal at these two temperatures, i.e., $M_S(5\text{ K}) \approx 153.2$ emu/g and $M_S(300\text{ K}) \approx 152.7$ emu/g, which is about 1.62 μ_B/Co atom. The value at 300 K decreases only slightly from the value at 5 K, and it is close to the bulk value of h-Co. A similar behavior has been observed with chains of submicron-sized Co hollow spheres, i.e., the saturation magnetization is almost independent of temperature from low temperature going up to $T =$ 395 K, see Figure 4 in ref 32. In addition, the property that $M_S(T)$ stays almost a constant for Co at $T < 300$ K is consistent with the result by theoretical analysis. For Co, $T_C = 1385$ K. The reduced spontaneous magnetization, $m(T/T_C) = M_S(T)/M_S(0)$, decreases by only about 1% from $T =$ 5 to 300 K.[33,34] In the low field region, open hysteresis loops

(26) Guo, F.; Zheng, H. G.; Yang, Z. P.; Qian, Y. T. *Mater. Lett.* **2002**, *56*, 906.
(27) Zheng, H. G.; Zeng, J. H.; Liang, J. H. *Acta Metall. Sin.* **1999**, *35*, 837.
(28) Zhang, X.; Xie, Y.; Xu, F.; Xu, D.; Liu, X. H. *Inorg. Chem. Commun.* **2004**, *7*, 417.
(29) http://math.nist.gov/oommf
(30) He, L.; Zheng, W. Z.; Zhou, W.; Du, H. L.; Chen, C. P.; Guo, L. *J. Phys.: Condens. Matter.* **2007**, *19*, 036216.
(31) Wang, N.; Guo, L.; He, L.; Cao, X.; Chen, C. P.; Wang, R.; Yang, S. *Small* **2007**, *3*, 606.
(32) He, L.; Chen, C. P.; Liang, F.; Wang, N.; Guo, L. *Phys. Rev. B* **2007**, *75*, 214418.

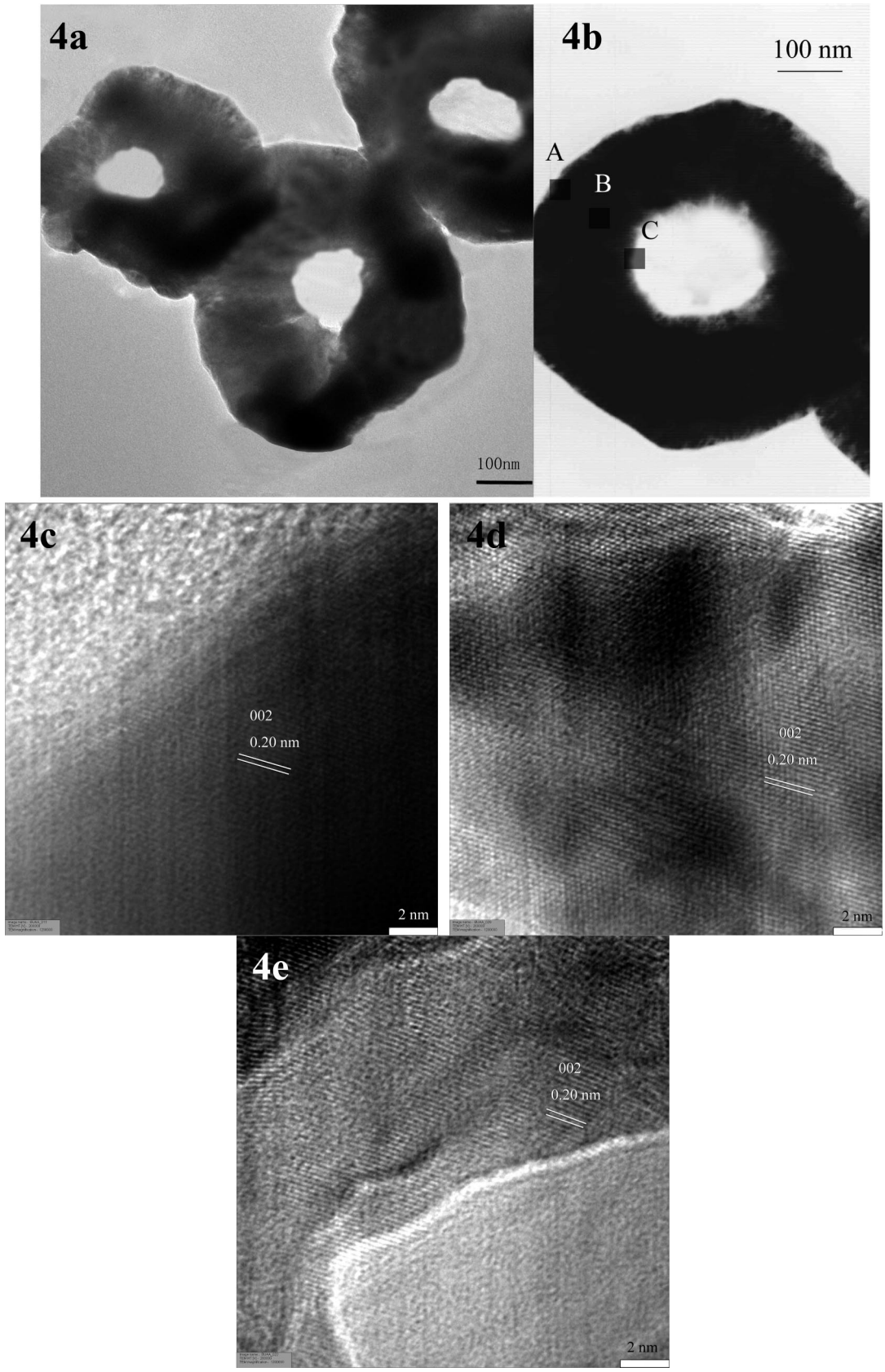

Figure 4. (a) TEM image of donut-shaped Co nanoparticles. (b) TEM image of a single typical donut-shaped Co nanoparticle. The HRTEM images for the surface of the Co ring on the (c) surface of the outer periphery, (d) side surface on the ring plane, and (e) surface on the interior of the ring.

are shown in the insets. At $T = 300$ K, the coercivity is determined as $H_C \approx 112$ Oe and the remnant magnetization is $M_R \approx 4.5$ emu/g. Interestingly, H_C, and M_R for the loop at $T = 5$ K are almost zero. A similar behavior has also been observed previously with Co submicrometer magnetic rings fabricated by high-resolution electron beam lithography and lift-off from cobalt thin films. Here the as prepared Co nanoring possessing outer diameter ~700 nm, inner diameter

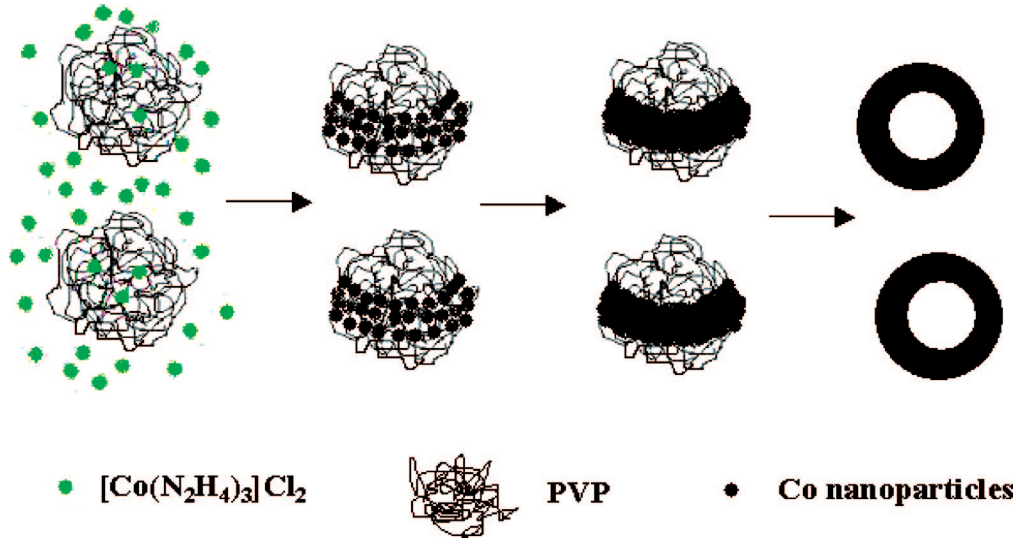

Figure 5. Formation of donut-shaped Co nanostructures.

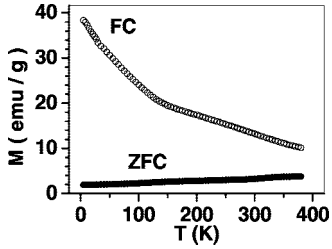

Figure 6. ZFC and FC curves measured in an applied field of 90 Oe between 5 and 380 K.

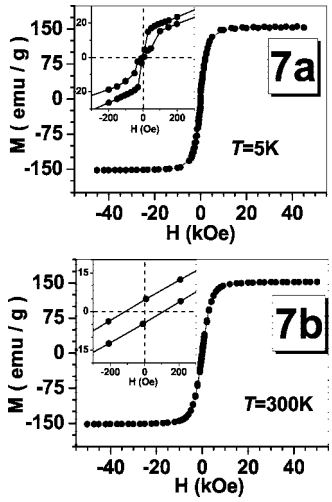

Figure 7. (a) $M(H)$ data measured at $T = 5$ K. The inset shows the open hysteresis loop in the low field region. (b) $M(H)$ data measured at $T = 300$ K. The inset shows the open hysteresis loop in the low field region.

~300 nm, and the lateral thickness ~ 50 nm.[35] It has been attributed to the vortex-curling magnetization state with this special ring-shaped geometry.[35–38]

To better understand this vortex-curling magnetization state, we have performed micromagnetic simulations using the OOMMF package[29] for the ground-state magnetic properties at $T = 0$ K. By taking into account the exchange energy, the anisotropy energy, the self-magnetostatic energy and the Zeeman energy within the ring, we have obtained an interesting feature for the $M(H)$ loop similar to that at $T = 5$ K, i.e., M_R and H_C are almost zero, see Figure 8. The simulation is performed by the time integration of the Laudau-Lifshitz-Gilbert equation. The magnetic properties of the bulk Co are used as the calculation parameters, i.e., the saturation magnetization, $M_s = 1.4 \times 10^6$ A/m, and the exchange stiffness constant, $A = 10.3 \times 10^{-12}$ J/m.[39] Because the sample is polycrystalline, the magnetocrystalline anisotropy has been neglected. In the calculation, the inter-ring interaction has been neglected as well. The geometric parameters used in the calculation for the nanoring are as follows, 400 nm for the outer diameter, 240 nm for the inner diameter, and 120 nm for the lateral thickness, i.e., the thickness of the ring plane. The default damping constant is set as 0.5. For the calculation, a cubic lattice with the cell size of $(10 \text{ nm})^3$ is selected. Although the dimension of the cell size is larger than the exchange length of Co, which is approximately equal to 3.37 nm,[35] for the reason of reducing the calculation time, the result turns out to be independent of the cell size. This is confirmed by an independent calculation using the cell size of $(8 \text{ nm})^3$, which gives the same calculated $M(H)$ curve. A similar treatment with a large cell size has also been adopted previously with success.[40] Because the experimental measurements were performed on the powder collection of randomly oriented nanoparticles, the measured hysterisis loop is of a statistically averaged property, which is different from that of the well-aligned

(33) Kuz'min, M. D. *Phys. Rev. Lett.* **2005**, *94*, 107204.
(34) Kuz'min, M.; Richter, M.; Yaresko, A. N. *Phys. Rev. B* **2006**, *73*, 100401.
(35) Li, S. P.; Peyrade, D.; Natali, M.; Lebib, A.; Chen, Y.; Ebels, U.; Buda, L. D.; Ounadjela, K. *Phys. Rev. Lett.* **2001**, *86*, 1102.
(36) Jung, W.; Castano, F. J.; Ross, C. A. *Phys. Rev. Lett.* **2006**, *97*, 247209.
(37) Castano, F. J.; Ross, C. A.; Eilez, A.; Jung, W.; Frandsen, C. *Phys. Rev. B.* **2004**, *69*, 144421.
(38) Neudecker, I.; Klaui, M.; Perzlmaier, K.; Backes, D.; Heyderman, L. J.; Vaz, C. A. F.; Bland, J. A. C.; Rudiger, U.; Back, C. H. *Phys. Rev. Lett.* **2006**, *96*, 057207.
(39) Skomski, R. *J. Phys.: Condens. Matter* **2003**, *15*, R841.
(40) Ziese, M.; Höhne, R.; Esquinazi, P.; Busch, P. *Phys. Rev. B* **2002**, *66*, 134408.

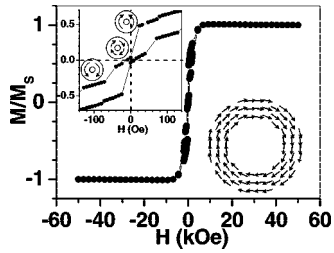

Figure 8. *M*(*H*) curve calculated by the OOMMF code. The upper left inset shows the loop in the low field region with the schematic figures describing the reversal process and the lower right inset shows a diagram for the vortex-curling magnetization state at zero field with in-plane field history calculated by OOMMF for the nanoring.

samples grown on the substrate.[41] To account for this point, a series of simulations have been performed by varying the direction of the applied field with respect to the ring plane from 0 to 90° with a step size of 10 degrees. The final hysteresis loop is obtained by averaging the above calculation results, and is shown in Figure 8. The shape of the calculated loop is similar to the *M*(*H*) curve of magnetization reversal for magnetic nanorings subject to an in-plane applied field.[41] For the *M*(*H*) measurement in the large applied field region, the magnetization configuration with the ring is in the bidomain "onion" state.[1] As the applied field decreases near $H = 0$, it turns into the vortex-curling state accompanied by an abrupt reduction of the magnetization in the *M*(*H*) curve. The characteristic field for the formation of the vortex-curling state is termed as the vortex nucleation field, H_N.[42] Its value is about 24 Oe by the present calculation, which is close to the experimental value of 28 Oe. A typical magnetization configuration of the vortex-curling state under the in-plane magnetic field obtained from the simulation is plotted in the lower right inset of Figure 8. This is consistent with the results reported previously.[35,40] By increasing the applied field in the negative direction from $H = 0$, a transition from the vortex-curling state to the onion state occurs at a critical field named the annihilation field, H_A.[42] It is 40 Oe according to the present calculation, which is not far off from the value of 30 Oe determined by the experiment.

At low temperature, the formation of a magnetization vortex-curling state with the submicrometer-sized Co rings is due to the donut-shaped or bracelet-like geometry. This corresponds to an energetic ground-state from the competition of the magnetostatic and exchange energy. For the formation of the magnetization vortex-curling state, an abrupt magnetization reversal occurs at the nucleation field, $H = H_N$, during the decreasing field in the *M*(*H*) measurement. It corresponds to an abrupt reduction in the magnetization, ΔM, at $H = H_N$ as shown in Figure 7a for the experiment or in Figure 8 for the calculation. The magnetization reversal is expected to proceed by a nucleation rotational mode with the spheriacal switching volume of Co estimated as $V^* = V_{coh} = \pi L_{coh}^3/6 = 1.8 \times 10^3$ nm^3, in which $L_{coh} \approx 15$ nm is the coherence length of Co.[39] The change in energy for the magnetization reversal at $H = H_N$ with the magnetic moment of the switching volume is estimated as $E_N = \Delta M V^* H_N$. Experimentally, $H_N \approx 28$ Oe and the corresponding $\Delta M \approx 10$ emu/g, the energy decrease for the formation of the vortex curling state is therefore calculated as $E_N = k_B T_{Nucl} \approx 32$ K, by using the experimental values for ΔM, H_N, and V^* explicitly. It indicates that at $T_{Nucl} = 32$ K, the step in the magnetization ΔM, at the nucleation field can be washed out by thermal energy. Therefore, at $T = 300\ \text{K} > T_{Nucl}$, the feature for the formation of the vortex curling state, which is an abrupt reduction in the magnetization, is not observed by the *M*(*H*) measurement.

Conclusions

To summarize, the donut-shaped Co nanomaterials are obtained via a solution phase synthesis method. The Co rings are characterized to have an outer diameter of about 400−500 nm in diameters and a ring thickness of about 120 nm. The coercivity at $T = 300$ K is about ten times of the bulk cobalt. At $T = 5$ K, the hysteresis loop exhibits a vanishing coercivity. This is attributed to the vortex-curling magnetization state at low temperature, as revealed by the Micromagnetic simulations for the magnetization ground state of a Co ring with the same size. The synthesis route is mild, high-yield, well-repeatable, low-cost, and easily controllable. Therefore, it represents an attractive path to large-scale assembly of metallic donut-shaped nanomaterials.

Acknowledgment. This project has been financially supported by the National Natural Science Foundation of China (20673009 & 50725208) and the State Key Project of Fundamental Research for Nanoscience and Nanotechnology (2006CB932300) as well as SRFDP-20060006005. Z.Y. Wu acknowledges the financial support of the Outstanding Youth Fund (10125523).

CM7025784

(41) Hayward, T. J.; Moore, T. A.; Tse, D. H. Y.; Bland, J. A. C.; Castaño, F. J.; Ross, C. A. *Phys. Rev.B* **2005**, *72*, 184430.
(42) Guslienko, K.Yu.; Novosad, V.; Otani, Y.; Shima, H.; Fukamichi, K. *Phys. Rev. B* **2001**, *65*, 024414.